Electronic Supplementary Information (ESI)

A simple strategy to achieve remarkable mechanochromism of cationic Ir(III) phosphors through subtle ligand modification

Kai-Yue Zhao,[a] Hui-Ting Mao,[a] Li-Li Wen,[a] Guo-Gang Shan,*[a] Qiang Fu,*[a] Hai-Zhu Sun[a] and Zhong-Min Su*[ab]

[a] *Institute of Functional Material Chemistry and National & Local United Engineering Lab for Power Battery, Faculty of chemistry, Northeast Normal University, Changchun, Jilin130024, P. R. China*

E-mail: shangg187@nenu.edu.cn (G. G. Shan), fuq863@nenu.edu.cn (Q. Fu), zmsu@nenu.edu.cn (Z. M. Su).

[b] *School of Chemistry & Environmental Engineering, Changchun University of Science and Technology, Changchun, Jilin 130012, P. R. China*

Table of Contents

Synthetic routes and characteristic of ancillary ligands L1-L4

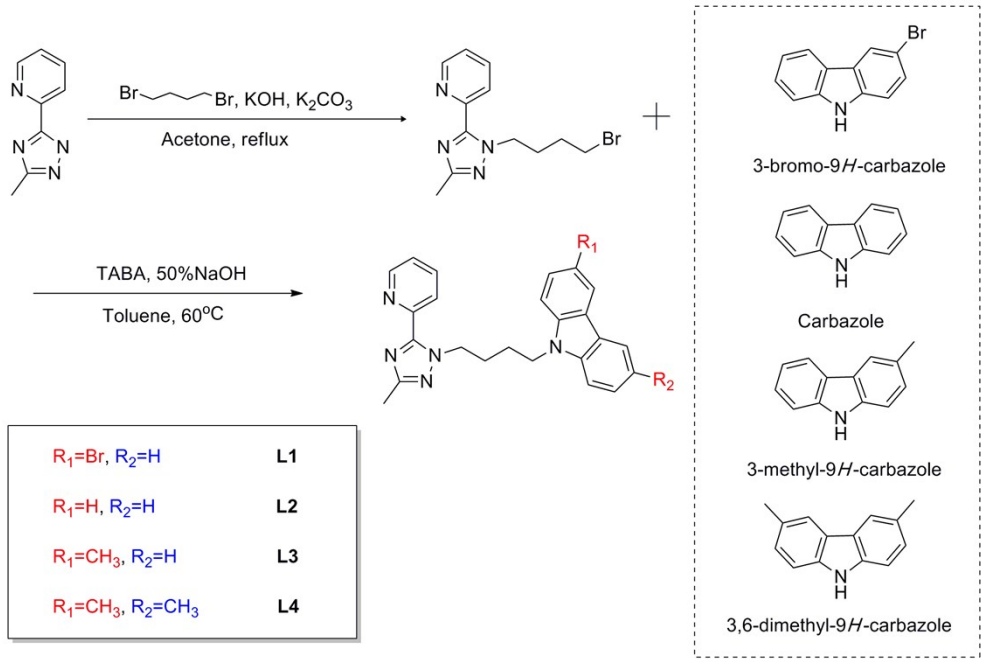

Scheme S1 Synthetic routes of the ancillary ligands **L1-L4**.

Scheme S1 exhibits the synthetic routes of the ancillary ligands **L1-L4**. 2-(3-methyl-1*H*-1,2,4-triazol-5-yl)pyridine, the intermediate **Inter-1** and ancillary ligand **L2**, **L4** were synthesized according to the modified reported procedures.[1, 2]

3-bromo-9-(4-(3-methyl-5-(pyridin-2-yl)-1*H*-1,2,4-triazol-1-yl)butyl)-9*H*-carbazole (L1).

Compound **L1** was prepared according to the procedure described for **L2**. Yield: 66%. ^{1}H NMR (500 MHz, $CDCl_3$, ppm): δ 8.53 (d, J= 4.5 Hz, 1H), 8.14–8.17 (m, 2H), 8.01 (d, J= 7.5 Hz, 1H), 7.80 (t, J= 7.5 Hz, 1H),7.44–7.50 (m, 2H), 7.37 (d, J= 8.5 Hz, 2H), 7.29–7.31 (m, 1H), 7.21–7.26 (m, 2H), 4.78 (t, J = 7.0 Hz, 2H), 4.30 (t, J = 7.0 Hz, 2H), 2.44 (s, 3H), 1.93–2.05 (m, 2H), 1.88–1.91 (m, 2H). MS (ESI): calcd for [$C_{24}H_{22}BrN_5$] ([M+H]$^+$) m/z 460.1137, found 460.1131. Anal. Calcd for $C_{24}H_{22}BrN_5$: C, 62.61; H, 4.82; N, 15.21. Found: C, 62.54; H, 4.75; N, 15.29.

3-methyl-9-(4-(3-methyl-5-(pyridin-2-yl)-1*H*-1,2,4-triazol-1-yl)butyl)-9*H*-carbazole (L3).

Compound **L3** was prepared according to the procedure described for **L2**. Yield: 68%. ^{1}H NMR (500 MHz, $CDCl_3$, ppm): δ 8.52–8.55 (m, 1H), 8.15 (d, J= 7.5 Hz, 1H), 8.04 (d, J= 7.5 Hz, 1H), 7.88 (s, 1H), 7.78–7.81 (m, 1H), 7.40–7.42 (m,1H), 7.34 (d, J= 8.5 Hz, 1H), 7.29–7.31 (m, 2H), 7.24–7.28 (m, 2H), 7.17–7.20 (m, 1H), 4.75–4.80 (m,

2H), 4.26–4.33 (m, 2H), 2.52 (d, J = 7.0 Hz, 3H), 2.44 (d, J= 3.5 Hz, 3H), 1.95–2.01 (m, 2H), 1.88–1.93 (m, 2H). MS (ESI): calcd for $[C_{24}H_{25}N_5]$ ($[M+H]^+$) m/z 396.2188, found 396.2183. Anal. Calcd for $C_{24}H_{25}N_5$: C, 75.92; H, 6.37; N, 17.71. Found: C, 75.85; H, 6.23; N, 17.80.

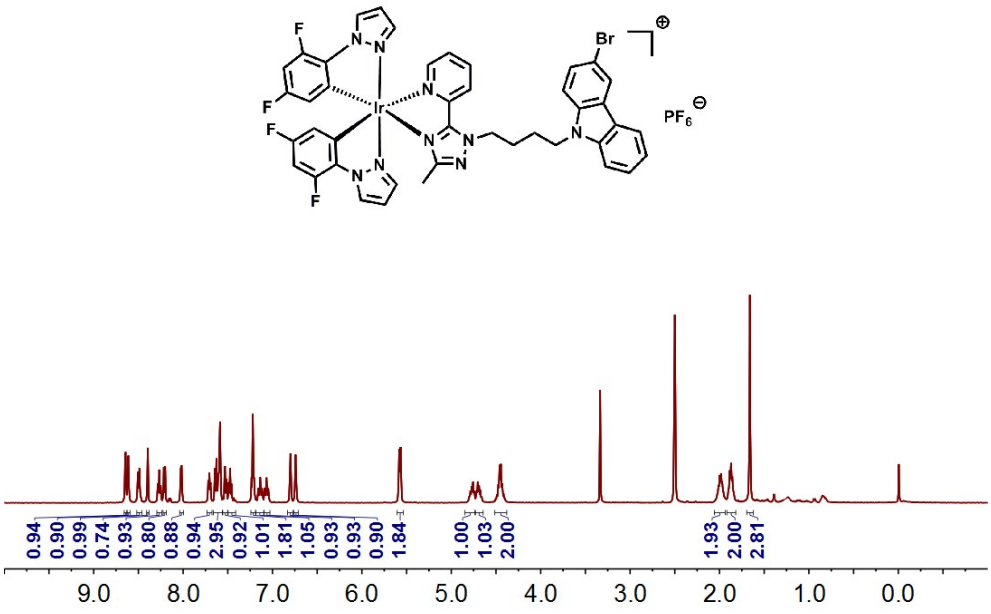

Fig. S1 ^{1}H NMR spectrum of **Ir-CzBr** in DMSO-d_6.

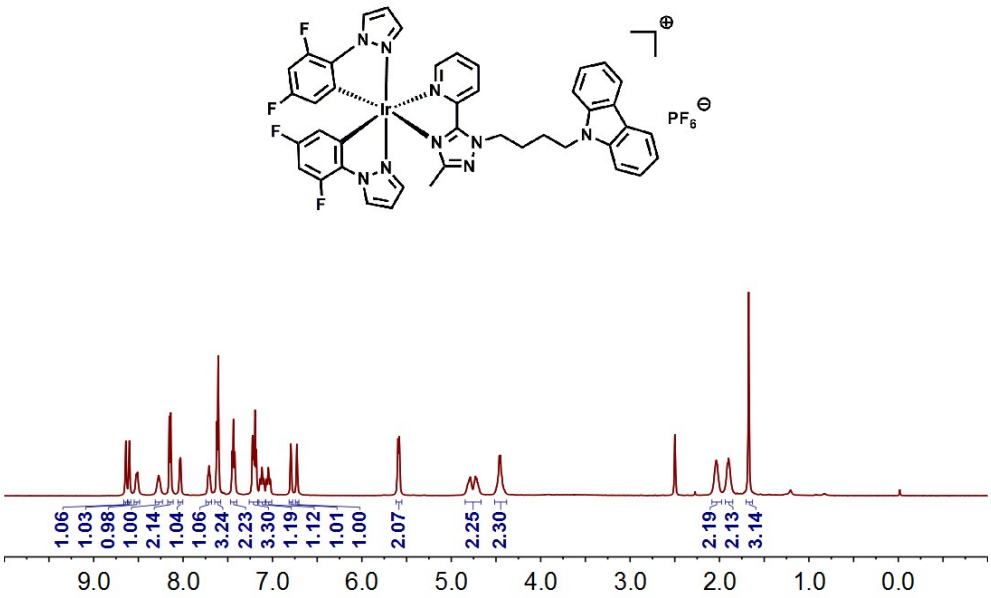

Fig. S2 ^{1}H NMR spectrum of **Ir-Cz** in DMSO-d_6.

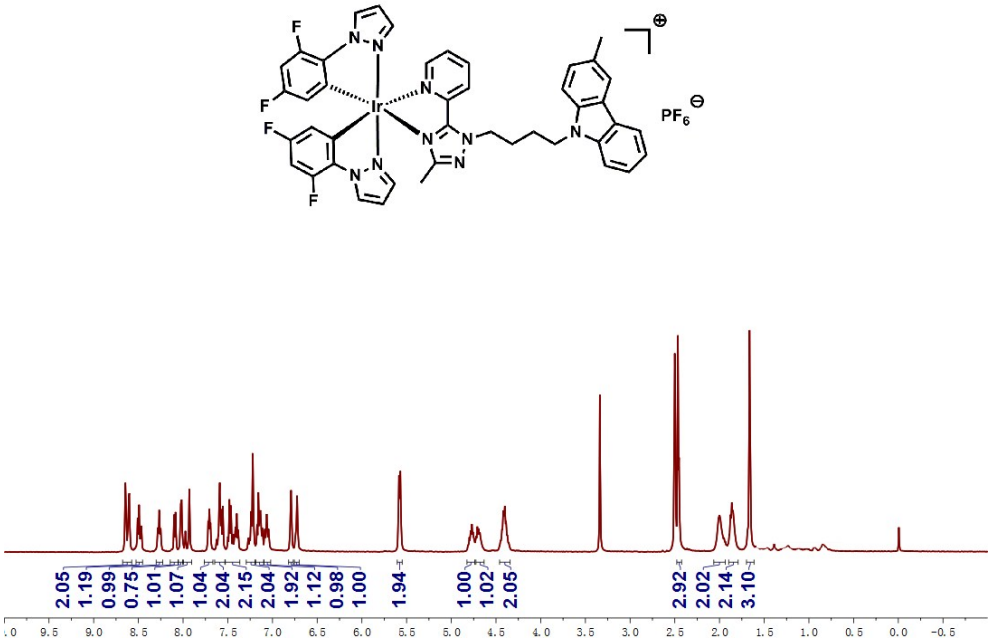

Fig. S3 [1]H NMR spectrum of **Ir-CzMe** in DMSO-d_6.

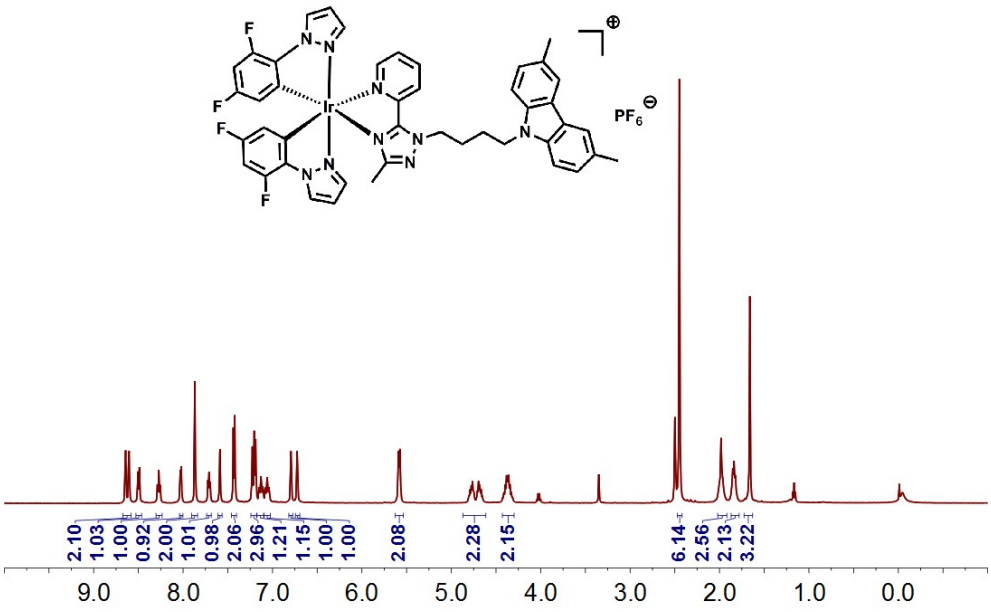

Fig. S4 [1]H NMR spectrum of **Ir-CzDMe** in DMSO-d_6.

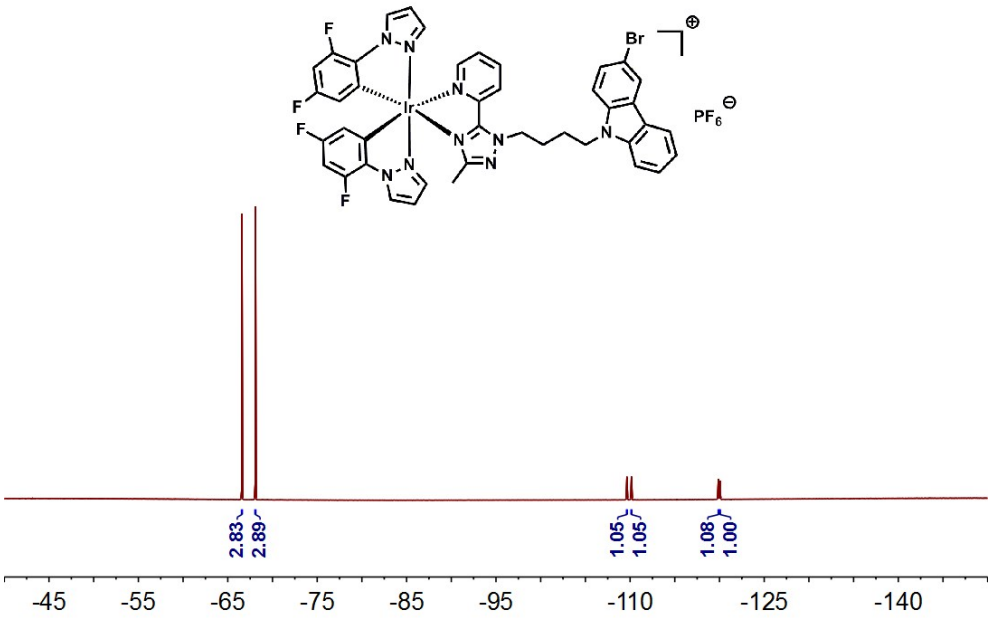

Fig. S5 ^{19}F NMR spectrum of **Ir-CzBr** in DMSO-d_6.

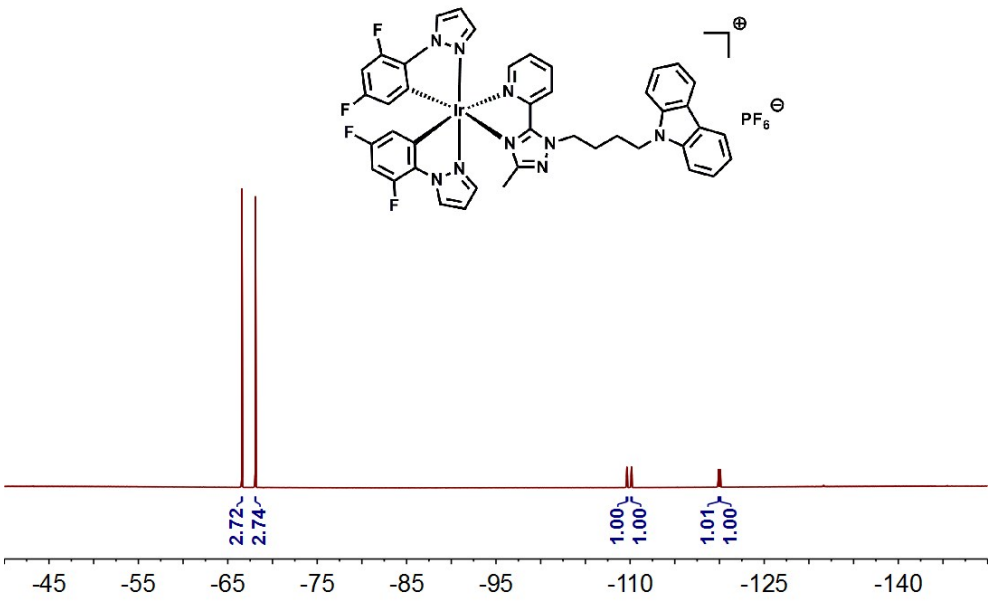

Fig. S6 ^{19}F NMR spectrum of **Ir-Cz** in DMSO-d_6.

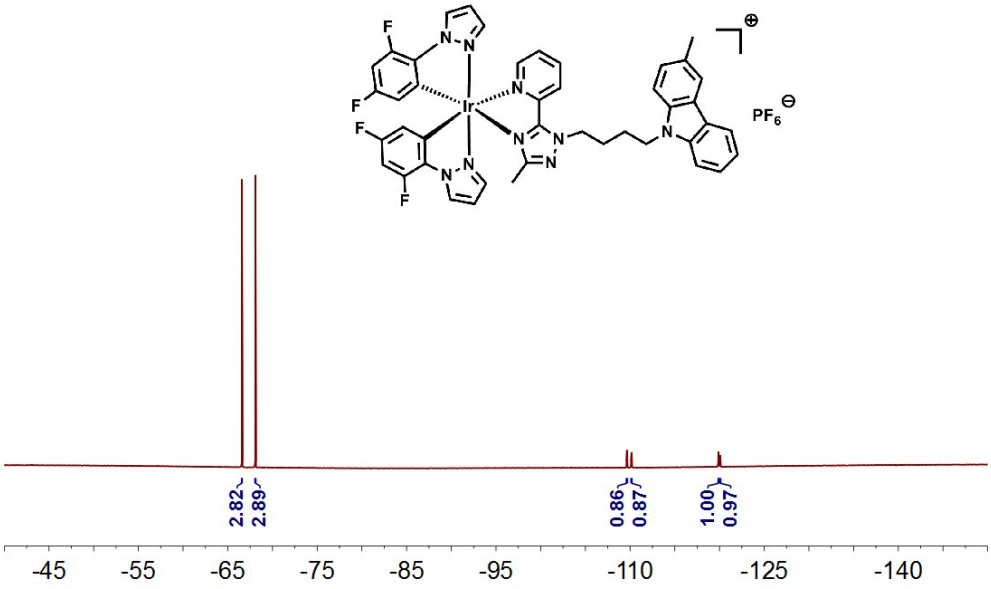

Fig. S7 ^{19}F NMR spectrum of **Ir-CzMe** in DMSO-d_6.

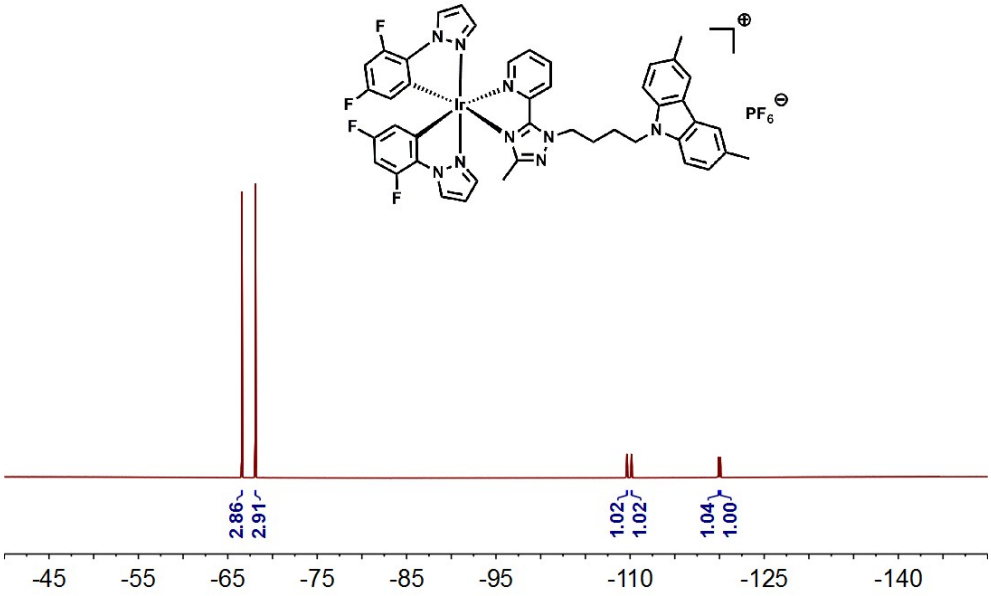

Fig. S8 ^{19}F NMR spectrum of **Ir-CzDMe** in DMSO-d_6.

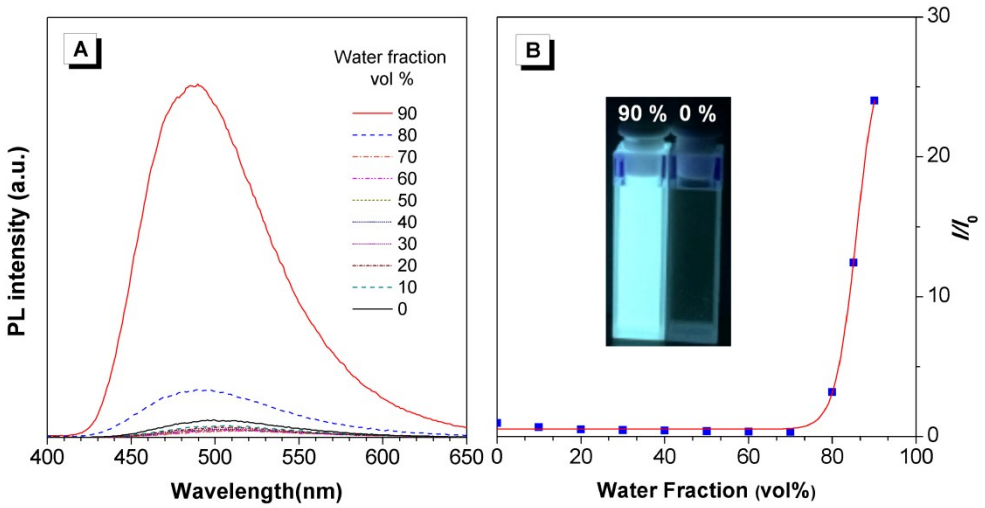

Fig. S9 (a) Emission spectra of **Ir-Cz** in CH_3CN-H_2O mixtures with different H_2O fractions (0–90%) at room temperature. (b) Plot of relative PL intensity (I/I_0) at 489 nm *versus* the composition of CH_3CN-H_2O mixture of **Ir-Cz**, where I_0 = peak intensity in pure CH_3CN. Inset: photographs of **Ir-Cz** in pure CH_3CN solution and CH_3CN-H_2O mixture (f_w = 90%) under 365 nm UV illumination.

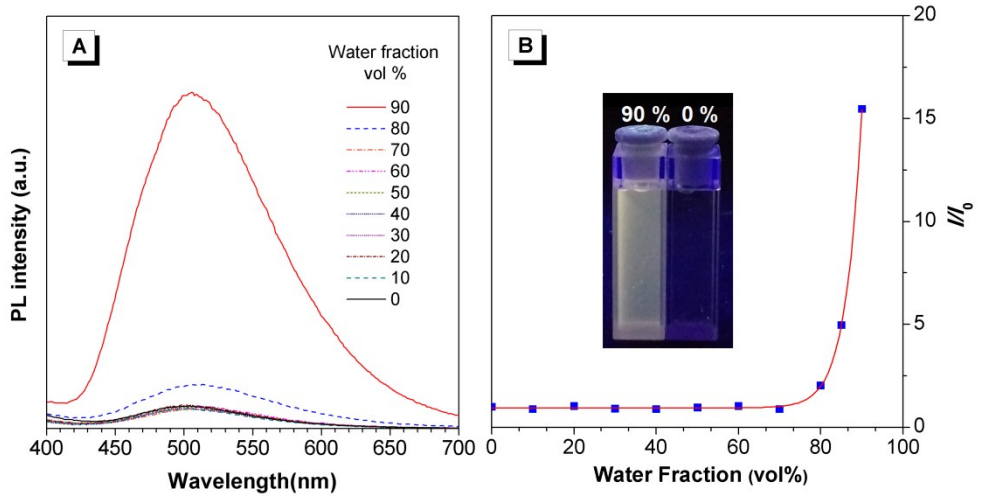

Fig. S10 (a) Emission spectra of **Ir-CzMe** in CH_3CN-H_2O mixtures with different H_2O fractions (0–90%) at room temperature. (b) Plot of relative PL intensity (I/I_0) at 508 nm *versus* the composition of CH_3CN-H_2O mixture of **Ir-CzMe**, where I_0 = peak intensity in pure CH_3CN. Inset: photographs of **Ir-CzMe** in pure CH_3CN solution and CH_3CN-H_2O mixture (f_w = 90%) under 365 nm UV illumination.

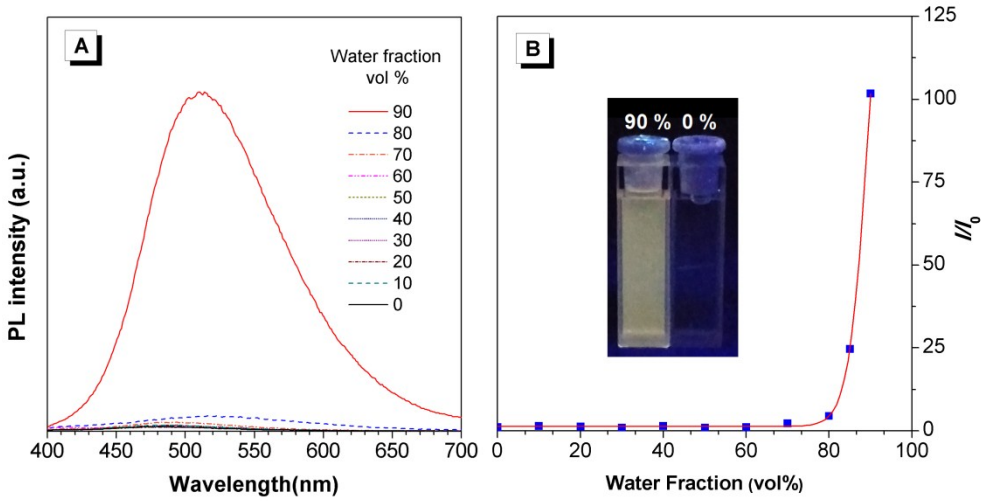

Fig. S11 (a) Emission spectra of **Ir-CzDMe** in CH_3CN-H_2O mixtures with different H_2O fractions (0–90%) at room temperature. (b) Plot of relative PL intensity (I/I_0) at 513 nm *versus* the composition of CH_3CN-H_2O mixture of **Ir-CzDMe**, where I_0 = peak intensity in pure CH_3CN. Inset: photographs of **Ir-CzDMe** in pure CH_3CN solution and CH_3CN-H_2O mixture (f_w = 90%) under 365 nm UV illumination.

Table S1 Photophysical characteristics of **Ir-CzBr**, **Ir-Cz**, **Ir-CzMe** and **Ir-CzDMe**.

	Solution	Solid		Neat film
	$\lambda_{em}{}^a$ (nm), $\Phi_F{}^b$ (%), τ^c (μs)	$\lambda_{em}{}^a$ (nm), $\Phi_F{}^b$ (%), τ^c (μs)	$\alpha_{AIE}{}^d$	$\lambda_{em}{}^a$ (nm)
Ir-CzBr	494, 1.0, 0.023	479, 33.3, 1.16	33.30	491
Ir-Cz	497, 0.5, 0.017	488, 23.8, 1.09	47.60	492
Ir-CzMe	503, 0.4, 0.028	498, 5.9, 1.20	14.75	510
Ir-CzDMe	488, 0.4, 0.038	516, 8.4, 0.28	21.00	538

[a] λ_{em}, emission maximum. [b] Φ_F, photoluminescence quantum yield measured by an integrating sphere. [c] τ, photoluminescence lifetime. [d] $\alpha_{AIE} = \Phi_F$(solid) / Φ_F(solution).

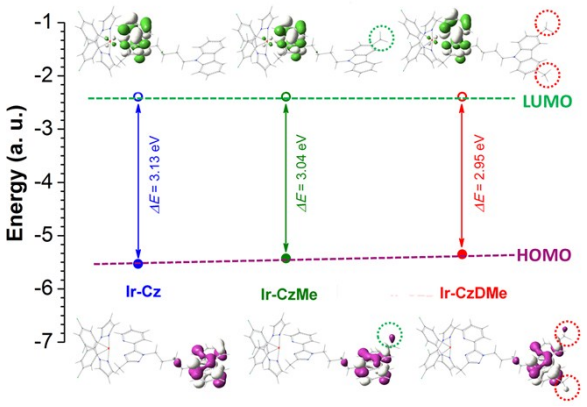

Fig. S12 Molecular orbital amplitude plots and energy levels of **Ir-Cz**, **Ir-CzMe** and **Ir-CzDMe**.

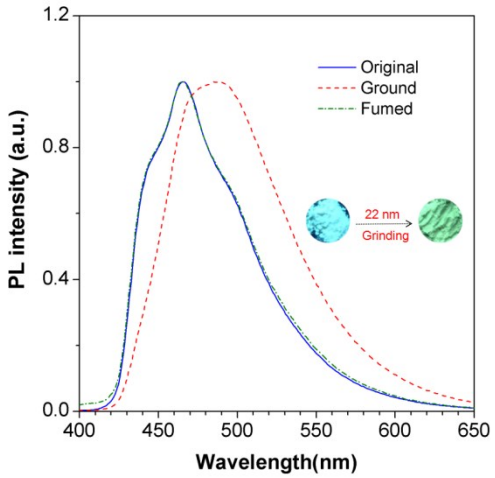

Fig. S13 Emission spectra of **Ir-Cz** in various states at room temperature. Inset: the photographs of **Ir-Cz** in various states under 365 nm UV illumination.

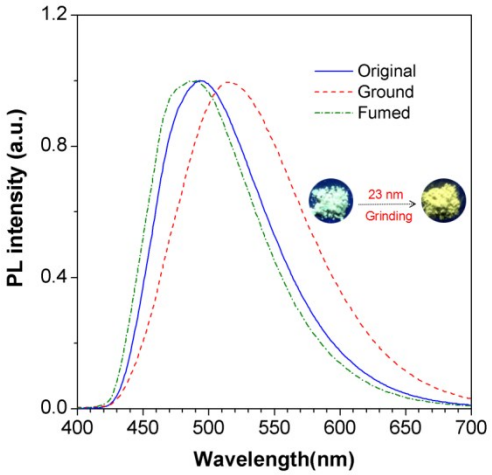

Fig. S14 Emission spectra of **Ir-CzDMe** in various states at room temperature. Inset: the photographs of **Ir-CzDMe** in various states under 365 nm UV illumination.

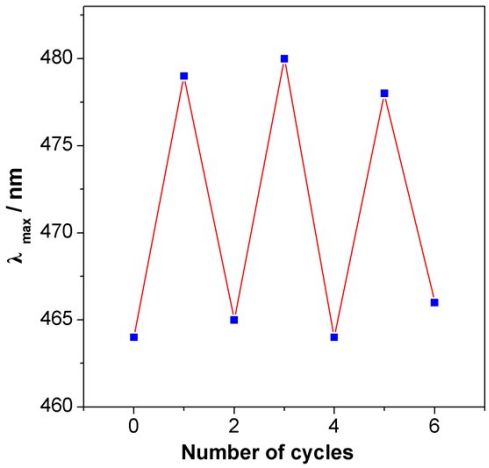

Fig. S15 Maximum emission wavelength changes of **Ir-CzBr** *versus* repeating cycles.

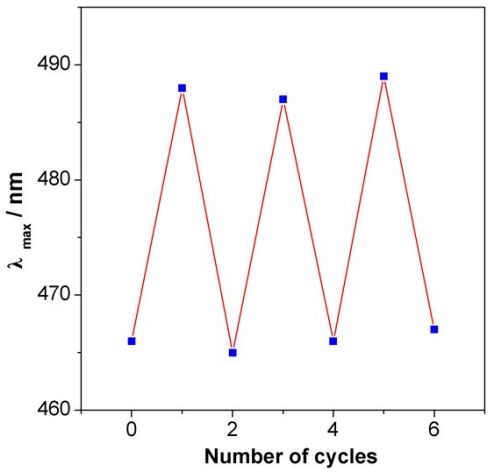

Fig. S16 Maximum emission wavelength changes of **Ir-Cz** *versus* repeating cycles.

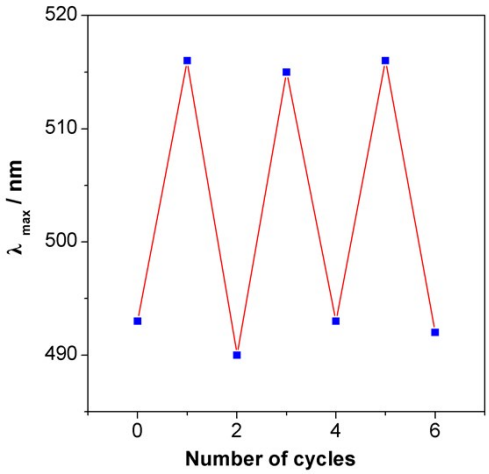

Fig. S17 Maximum emission wavelength changes of **Ir-CzDMe** *versus* repeating cycles.

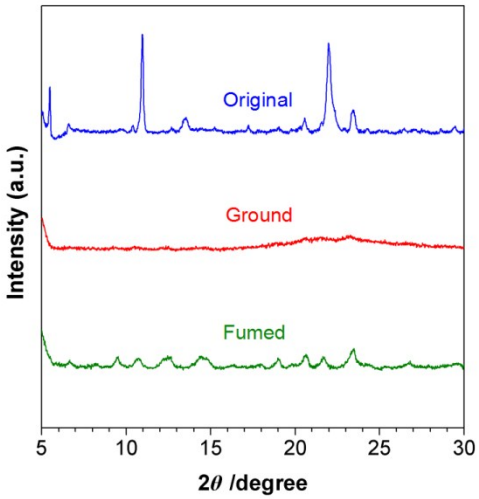

Fig. S18 Powder X-ray diffraction patterns of **Ir-CzBr** in various states.

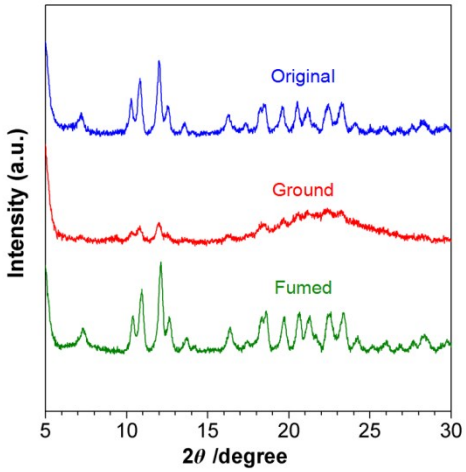

Fig. S19 Powder X-ray diffraction patterns of **Ir-Cz** in various states.

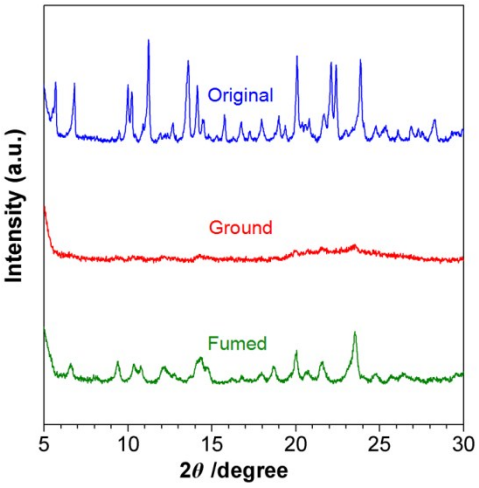

Fig. S20 Powder X-ray diffraction patterns of **Ir-CzDMe** in various states.

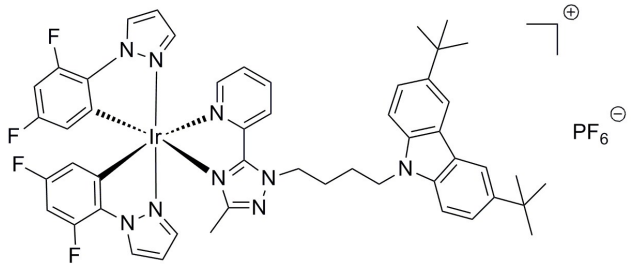

Fig. S21 Chemical structure of **Ir-CztBut** reported in Ref. 2.

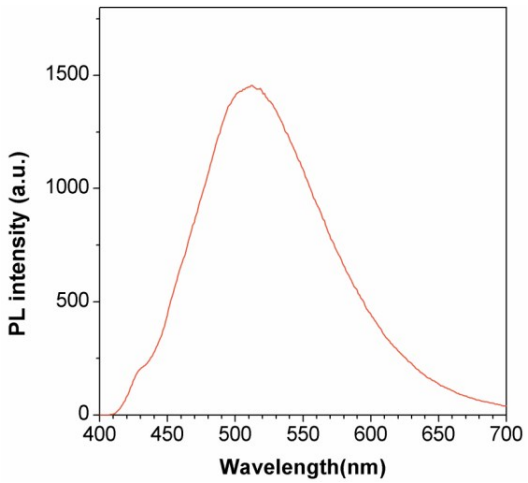

Fig. S22 The emission spectrum of **Ir-CztBut** in powder at room temperature.

References

1. K.-Y. Zhao, G.-G. Shan, Q. Fu and Z.-M. Su, *Organometallics*, 2016, **35**, 3996.

2. G.-G. Shan, H.-B. Li, H.-Z. Sun, D.-X. Zhu, H.-T. Cao and Z.-M. Su, *J. Mater. Chem. C,* 2013, **1**, 1440.